J. Fluid Mech. (1996), *vol.* 324, *pp.* 25–54

Molecular diffusion and viscous effects on concentration statistics in grid turbulence

By MICHAEL S. BORGAS AND BRIAN L. SAWFORD
CSIRO Division of Atmospheric Research, Aspendale, Victoria 3195, Australia

(Received 21 December 1994 and in revised form 24 April 1996)

Two-particle Lagrangian models in turbulence are used to consider dispersion in decaying isotropic homogeneous turbulence (i.e. approximating grid-generated wind-tunnel flows). Thomson's formulation is used, and his model is extended to incorporate molecular diffusivity and viscosity, i.e. the range of scales modelled includes the dissipation subranges as well as the inertial subrange. New terms are proposed which consistently provide well-mixed models and the impact on Saffman's well-known small-time results is considered. The new model is ideal for comparison with recent concentration-fluctuation measurements in decaying wind-tunnel turbulence and the results are encouraging. In particular, the fluctuation intensities, both along and across the wind tunnel, are well described by the new model. In addition, small source-size effects are far better explained when we include the molecular effects. A surprising result is the persistence in time of both source-geometry and molecular effects upon concentration fluctuations. Both of the effects are negligible at large times for mean concentrations, but persist for significant times for the fluctuations, indicating an important role for small-scale dynamics.

1. Introduction

Thomson (1990) has provided a Lagrangian technique for estimating the spatial and temporal development of concentration fluctuations in turbulent flows for arbitrary initial scalar fields. The method is particularly suitable for examining dispersion from compact initial sources rather than homogeneous random initial fields, when perhaps Eulerian methods are more suitable (Sinia & Yakhot 1989), although Lagrangian ideas have been used for this problem as well (Nelkin & Kerr 1981; Durbin 1982). Kaplan & Dinar (1988) provide an alternative Lagrangian technique, but we choose only to consider Thomson's.

Here we examine the dispersion appropriate for wind-tunnel flows where the scalar field is heat and the source is a heated wire of small diameter. The problem is to describe the ensuing scalar field: first, its spatial mean-temperature pattern and, secondly, its spatial temperature-fluctuation pattern. We suppose that the source is heated constantly and that the downstream statistics are therefore stationary. Below we use a model based on the concept of passive material particles (say molecules) for the scalar field.

We uniformly use concentration as the descriptive measure of the scalar field, though when we consider measurements, the field is of temperature. We thus also assume that thermal dispersion and material dispersion are effectively equivalent when the respective thermal and molecular diffusivities are the same.

The model we use (as adapted from Thomson) is a two-particle model and provides

only the first two moments of the scalar field. Therefore the results we obtain provide only a small part of the information contained within the probability density function for scalar concentration, but nevertheless they are important characteristics. In fact, in air-pollution studies it is seldom that characteristics other than the mean are considered, but we hope to advocate increased awareness of the role of higher moments and provide tools with which to estimate these moments, particularly in the context of the atmospheric boundary layer.

One-particle Lagrangian models are widely used in atmospheric pollution studies for the purpose of estimating mean-concentration fields. For such models, the crucial step is the appropriate parameterization of the energy-containing scales of the turbulence (and the mean flow) and these are often taken from mesoscale numerical models. The methods developed over the years are useful in practical, even regulatory, ways and in general mean concentration fields are understood relatively well.

Particle-pair trajectories sample turbulence rather differently, however, than do single-particle trajectories (Borgas & Sawford 1991) and two-particle models are necessarily more complicated. Because we consider compact sources, it is inevitable that we must consider particles that are close together in a single realization of the flow. The rate at which these particles separate is crucial in determining how fast the mixing occurs and thus the level of fluctuations. Consequently, a great deal of the importance of a two-particle model attaches to the small-scale properties of the turbulence and, to better understand the precise role played by turbulence, it is worthwhile considering simpler flows than those typically encountered in the atmosphere. Even then, the small-scale separation behaviour is not understood very well. In addition, the controlled measurements that we need to compare our theory with experiment only exist in the laboratory (wind tunnel) in enough detail for a comprehensive test. Such flows are designed to be idealized approximations and are of much lower Reynolds number than flows in the atmosphere. Thus the small-scale properties of laboratory experiments and atmospheric flows are not necessarily alike; nevertheless both flows are complex and mixing.

Wind-tunnel flows are also in the realm of direct numerical simulations of turbulence and hence of simulated scalar mixing too (Yeung & Pope 1989). However, it is inconceivable that direct numerical simulations will extend to atmospheric flows in the near future so that some degree of modelling is inevitable. Our purpose here is to develop a two-particle model, i.e. an acceptable approximation to reality, that agrees with wind-tunnel measurements, but which can be extended to flows of much greater complexity and structure. Such a model depends on the Reynolds number and we wish to vary this parameter over orders of magnitude: from 'low' values appropriate for laboratory experiments to arbitrarily large values appropriate for the atmosphere.

Pope (1994) gives the most comprehensive and up-to-date account of Lagrangian stochastic models for transport studies. Here we consider only a small part of this broad topic and focus upon Thomson's (1990) two-particle model. This model was developed on the premise of arbitrarily large Reynolds number and resolves scales only within the inertial subrange. The justification for the Markovian nature of this model essentially depends on infinite Reynolds number (Borgas & Sawford 1991, 1994*a*). The extensions we make, by incorporating molecular diffusion and viscous dissipation ranges, are *ad hoc* and only defensible by virtue of good comparisons with experiments and, indeed, are essential for that purpose. The Markovian basis for Thomson's model is not compromised by molecular diffusion (but the transport of material is not now solely by fluid-particle advection). However, it is inconsistent to include dissipation ranges in the context of a Markovian model for velocity and displacement of material

particles because viscous effects clearly have a memory according to a dissipative time scale.

Sawford (1991) has shown how a Markovian process for acceleration, velocity and displacement can incorporate dissipative ranges for one-particle Lagrangian statistics. Importantly, Sawford shows that the effect of finite Reynolds number is to set an effective value for the universal constant C_0 which will be encountered below. The complexity of generalizing two-particle models to such higher-order auto-regressive processes prohibits their use in a practical way. Here we include dissipation ranges essentially to modify the Eulerian structure functions for the velocity field, which, for the wind-tunnel flows we consider, do not display inertial ranges. We assume that for the Reynolds numbers encountered here, the dominant effect of viscosity is to modify the structure functions and that the stochastic equations used are essentially inviscid (perhaps allowing for the parameters to account for finite Reynolds numbers). The encouraging results obtained using this procedure provide some justification. It should be remembered that the aim is to find a model that can explain features of the experiments (at least not be in gross conflict with them), but which can then be adapted for use in the atmospheric boundary layer. In this case, the Reynolds numbers and Péclet numbers become so large that the neglect of viscous effects and molecular diffusion is no longer an issue.

Borgas & Sawford (1994*a*) have considered defects in Thomson's model because there is no account of intermittency. However, the conclusion there is that, at least for dispersion quantities, the effect of intermittency is rather small and unlikely to change the results significantly. Similarly, Borgas & Sawford (1994*b*) have considered a more general class of models which are essentially like Thomson's but which can be chosen to have some additional dynamical properties by explicitly considering the pressure calculated from the Navier–Stokes equation for prescribed velocity statistics. Again, the effect upon dispersion is not strong and Thomson's model remains perhaps the simplest model satisfying several robust modelling criteria.

In our work, as in Thomson's, we use the approximation that the Eulerian distribution of fluid velocities is Gaussian. Although this is certainly flawed, the results obtained suggest that it does not impact very much on dispersion (in grid turbulence). Here we aim for the simplest extension of Thomson's model and therefore choose to ignore the more complicated versions that exist, but we anticipate that the qualitative trends that emerge will be general, i.e. molecular diffusion will always facilitate particle separation while viscous subranges will slow down separation (when the particles are close enough together).

In §2 of this paper we briefly describe Sawford & Tivendale's (1992) experimental set-up, the experimental parameters and some approximations that we believe facilitate modelling.

In §3 we outline Thomson's two-particle model for self-similar decaying turbulence which is both homogeneous and isotropic. We also relate the concentration statistics to given two-particle displacement statistics and demonstrate that the need to account for molecular effects.

In §4 we generalize Thomson's model to allow for a parameterization of the influence of viscosity and molecular diffusion. One important change in character is that self-similar decay of the turbulence restricts the power-law exponent (of kinetic energy say) to a single value when viscous parameterization is included. However, the experimental data consistently predict a different exponent, with the implication that as time proceeds the extent of the dissipation range grows relative to the other lengthscales in

the problem. While this is no real difficulty, it requires more extensive numerical calculations to derive the concentration statistics as functions of time.

The generalization also requires a reassessment of the 'well-mixed' criterion of Thomson (1987, 1990). In order to simply satisfy this fundamental constraint, an expedient term is included in the statistical advection equation which is strictly unphysical, but successful computation suggests that the distortions are negligible for weak enough molecular diffusion.

The final version of the model (again with parameters selected to best model the mean concentration) is then used in §5 to predict spatial concentration fluctuations which are compared with the experiments. It is clear that the trends imposed by the modelling of dissipation ranges, together with molecular diffusion, largely explain the differences between the measured and modelled concentration fluctuations.

In §6, a comparison is made between the present model and Saffman's (1960) results. He used an expansion procedure to examine the small-time behaviour of turbulent diffusion, focusing on the role of molecular diffusion. Like Sawford & Hunt (1986), we hope to model turbulent diffusion for much longer times than for which Saffman's analysis holds. Nevertheless, our model should be interpreted in the context of the behaviour described by Saffman (1960).

In §7, the implications for modelling in the atmosphere (at least for Reynolds and Péclet numbers appropriate for the atmospheric boundary layer) are discussed by examining model predictions for a sequence of ever higher Reynolds number. It is clear that the results asymptote toward the original results of Thomson (1990), i.e. the results for large Reynolds numbers smoothly asymptote towards the infinite-Reynolds-number limit. In fact, when the Reynolds number is of order 10^5, the results are essentially inviscid, although this depends on the source characteristics. The present stochastic-modelling tool is specifically developed with a view to eventual application in atmospheric flows, which are not amenable to direct simulation when the effects of small inertial-range scales are important. We stress again that the stochastic equation we have used is not proposed as the best and most well-founded method for dealing with low-Reynolds-number flows, although it seems to produce reasonable results. The reason for constructing the model was that no sufficiently reliable data set exists for concentration fluctuations in large-Reynolds-number flows and that in order to make any comparison at all of theory and experiment we must limit ourselves to the present regime.

Discussion and conclusions are given in §8.

2. Wind-tunnel dispersion experiments

Sawford & Tivendale (1992) have conducted experiments over a number of years at CSIRO's Division of Atmospheric Research, essentially carefully repeating and expanding the experiments of Townsend (1954), Uberoi & Corrsin (1952), Warhaft (1984) and Stapountzis *et al.* (1986). A small suction wind tunnel with grid-generated turbulence and uniform mean flow is seeded with passive heat tracer by a thin wire placed horizontally across the tunnel downstream of the grid in fully developed turbulence. Of course the turbulence is not strictly homogeneous (or isotropic) because it decays with downstream distance. However, in a frame of reference moving with the mean flow, the flow appears instead to be non-stationary (with decaying turbulent kinetic energy, for instance) and, at least locally, the variations of flow statistics in the mean-flow direction are negligible. The turbulent transport that concerns us seldom exceeds a few centimetres (except perhaps far downstream of the source), so that

relative to the size of the wind-tunnel (3 m long with a 0.69×1.02 m^2 cross-section) the 'localized' nature of dispersion is ensured. Therefore, it is entirely reasonable to use the transformation to homogeneous but decaying turbulence. Similarly, the turbulence will be assumed to be isotropic.

In the moving frame, the continuous heat source appears to recede from the dispersion domain. However, we shall approximate the dispersion problem by assuming that at some instant an area source gives an impulse of heat which then diffuses and mixes in the vertical. This approximation is good because the mean flow velocity U is so large, 500 cm s^{-1}, while the intensity of the turbulence is small, approximately 5%. Thus, we effectively ignore the longitudinal mixing.

Other parameters of note are the source-wire diameter, $d = 0.02$ cm; downstream location of the source, $x_0 = 31$ cm; and velocity fluctuation at the source, $\sigma_u^2 = \chi U^2$, where $\chi = 0.29 \times 10^{-2}$. The dynamics of the turbulence are assumed to be approximately self-similar, i.e. look identical at each downstream location with the appropriate definition of scale. Such decay is often measured so that, for example, the turbulence kinetic energy decays with downstream distance (x) as

$$\sigma_u^2 = \chi U^2 (x/x_0)^{-2m}, \tag{2.1}$$

for some decay exponent m. Sawford & Tivendale's measurements give $m = 0.7$, which is at the upper end of the range of values from other experiments. Note that this decay is only self-similar with respect to inviscid scales and the extent of the viscous dissipation range grows with downstream distance. If $m = 0.5$, then the motion is statistically self-similar on all lengthscales, i.e. the integral lengthscales and dissipative lengthscales grow at the same rate with downstream distance; correspondingly, the velocity fluctuations become smaller and the Reynolds number remains constant. However, the experiments are decisive in precluding $m = 0.5$ from experimental relevance.

Self-similarity is useful because it facilitates the computation of dispersion statistics. For infinite-Reynolds-number models, i.e. ignoring the dissipation ranges, it is possible to use self-similarity to our advantage and effectively compute all the necessary dispersion statistics from one evolution in time. By this we mean that, in general, we are concerned with two-time statistics: the time of release of tracer and the time we record a tracer concentration. In decaying turbulence, the absolute value of both these times is significant but with self-similarity a single effective lag becomes the significant time. For models with explicit dissipation ranges, self-similarity when $m = 0.5$ allows the same simplification, but as this is not relevant for practical wind-tunnel flows, it is generally necessary to explore the two-time space of dispersion, which is computationally more intensive.

The inhomogeneous stationary flow represented by the wind tunnel can be replaced by an approximate homogeneous non-stationary (decaying) flow by considering the frame of reference moving with the mean flow. Let t_0 be the elapsed time for the advection of the mean flow from the grid to the source location, i.e. $x_0 = Ut_0$. At time $t = 0$ we define the (x, z) origin of the moving frame to coincide with the heat source (i.e. the y-axis). Then the turbulence seen in the moving frame for subsequent times apparently decays, e.g. the velocity fluctuations decrease like

$$\sigma_u^2 = \chi U^2 \left(1 + \frac{t}{t_0}\right)^{-2m}, \tag{2.2}$$

and moreover the flow is approximately homogeneous and isotropic, at least in the neighbourhood of the origin.

The local lengthscale of the turbulence is intrinsic and is determined by other scales of the turbulence (near the grid it must be anticipated that the lengthscale is related to mesh size, but farther downstream the scales are self-determining). The mean energy dissipation rate (per unit mass) in the moving frame is given by

$$\bar{\epsilon} = -\frac{3}{2}\frac{\partial \sigma_u^2}{\partial t} = 3m\chi t_0^{-1} U^2 \left(1+\frac{t}{t_0}\right)^{-2m-1}. \tag{2.3}$$

The local structure of the turbulence is often described with respect to the parameters σ_u and $\bar{\epsilon}$ to the extent that the lengthscale of velocity fluctuations is given by

$$L \sim \frac{\sigma_u^3}{\bar{\epsilon}} = \frac{1}{3m}\chi^{1/2} U t_0 \left(1+\frac{t}{t_0}\right)^{1-m}. \tag{2.4}$$

Since the general estimates for m are less than one, we see that as the turbulence decays the velocity fluctuations get smaller and the lengthscale over which they are correlated gets larger. The Reynolds number based on these intrinsic scales is

$$Re = \frac{\sigma_u L}{\nu} = \left(1+\frac{t}{t_0}\right)^{1-2m} Re_0, \tag{2.5}$$

where ν is the kinematic viscosity (of the air) and $Re_0 = (1/3m)\,\chi(Ux_0/\nu)$ is the Reynolds number at the source. Note that, unless $m = 0.5$, the Reynolds number changes with time (downstream location). Because the experimentally determined value is $m \approx 0.7$, the Reynolds number becomes continuously smaller in time.

Similarly, the Péclet number appropriate for molecular (thermal) diffusion, with molecular (thermal) diffusivity κ, is

$$Pe = \frac{\sigma_u L}{\kappa} = \left(1+\frac{t}{t_0}\right)^{1-2m} Pe_0, \tag{2.6}$$

which changes with time, from the source-location value Pe_0, unless $m = 0.5$. In the experiments the tracer is heat and the temperature near the source is high (~ 350 °C), thus the model of molecular diffusion should account for the fact that κ is larger near the source than farther downstream with cooler ambient temperatures. On the other hand, the heat tracer is essentially passive so that the structure of the turbulence (in particular the dissipation range) is not affected. We account for temperature effects in the molecular diffusion but ignore them in the viscous effects; therefore the model uses an effective Prandtl number of about 0.5 (i.e. a bulk representative temperature of about 100 °C is used to estimate κ). Note that we fix this number for all time. As molecular mixing intermingles cooler ambient air with the heated air, thereby lowering the temperature, the appropriate Prandtl number will decrease.† However, this should only happen some distance downstream and, because we find only minor impact of molecular diffusion far from the source and because we cannot model the temperature dependence correctly with our two-particle stochastic models, we shall not endeavour to improve upon the simplistic idea used above (i.e. we essentially model molecular diffusion correctly near the source but not elsewhere).

For the present circumstances, the relevant physical parameters near the source location of $x = 31$ cm (denoted with subscript zero) are

$$\sigma_{u_0} = 26.7 \text{ cm s}^{-1}, \quad L_0 = 0.79 \text{ cm}, \quad Re_0 = 144, \quad Pe_0 = 62, \quad \sigma_0 \sim 0.02 L_0.$$

† Turbulent mixing of fluid particles does not directly intermingle air particles and it is often assumed that the heat (concentration) in a fluid particle remains the same indefinitely at large Péclet numbers.

The source-size parameter, σ_0, which is the spread of an assumed Gaussian-shaped source, remains uncertain because no explicit account is taken of thermal boundary layers immediately adjacent to the heated wire. The scale of these effects is in any case similar to the turbulence dissipative lengthscales

$$\eta \sim L_0 Re_0^{-3/4} = 0.025 L_0$$

so that no strong dependence upon σ_0 is expected in this range. Only when the lengthscale of concentration variations is significantly larger than η are the fluctuations affected significantly by the turbulence, i.e. a highly localized blob moves as one until its size is larger than dissipation scales and then it is rapidly distorted.

Thus the model we need must accommodate moderately large Reynolds-number effects (with Taylor-scale Reynolds number $Re_\lambda = (15Re)^{1/2} \sim 45$), and must resolve very small source size characteristics, i.e. many different lengthscale processes contribute to the dispersion. The tunnel is approximately 3 m long so that t/t_0 of order 10 is the maximum elapsed experimental dispersion time. An estimate when $t \gg t_0$ for the root-mean-square lateral excursion of a particle initially on the centreline is (Thomson 1990)

$$L_0\left(2Pe^{-1}\left(\frac{t}{t_0}\right)+\frac{3m}{(1-m)(1-m+\frac{3}{2}mC_0)}\left(\frac{t}{t_0}\right)^{1-m}\right)^{1/2}, \tag{2.7}$$

which reaches about 5 cm at the end of the tunnel, but is less than 2 cm for the first half of the tunnel.

These parameters will guide the modelling principles for the remainder of the paper. Although it is certain that inertial-range effects are obscured because of the low Reynolds number, it is likely that a useful model will be based on corrections to a high-Reynolds-number formulation, i.e. the basic mechanics of the wind-tunnel flow will qualitatively be those of typical turbulence. The model must also be able to resolve at least three orders of magnitude in lengthscale and calculate velocity and scalar fields for ten or more eddy-turnover times. Clearly, this represents a major computational exercise but is feasible using modern Lagrangian techniques.

3. Two-particle stochastic models: Thomson's model

In this section we compare Thomson's model predictions of concentration fluctuations with Sawford & Tivendale's (1992) results. This comparison shows that the modelled fluctuations are generally unreasonable and are only partially remedied by using an effective source size, many times the source size of the experiments. There are also problems with the small-time behaviour and overall the comparison is not very good but we will attempt to explain the discrepancies that exist. First, we give the formal description of the concentration fluctuations in terms of the probability density for particle pair displacements (§3.1). Then Thomson's (1990) model is outlined and discussed, and finally some results of calculations with this model is given (§3.2).

3.1. *Two-particle concentration statistics*

The transport of material can be usefully described in Lagrangian terms. Suppose that a material particle is located at position y at time s (this could be the source). Heat transport is a more difficult concept in the Lagrangian context and we simply assume exact correspondence between the transport of heat and the transport of (say) tracer molecules when the thermal diffusivity and molecular diffusivity are the same.

Macroscopic material blobs are made up of many material particles and the motion of the blob requires the joint instantaneous description of each particle. A simpler goal is the calculation of ensemble-average moments of the material concentration field. Following Sawford & Hunt (1986), if the instantaneous source concentration at time s is $S(\boldsymbol{y})$, then at time t ($t > s$) the ensemble-average spatial structure of the material concentration field at position $\boldsymbol{x}$ is given by

$$\langle C(\boldsymbol{x}, t)\rangle = \int P_1(\boldsymbol{x}, t\,|\,\boldsymbol{y}, s)\, S(\boldsymbol{y})\, \mathrm{d}^3\boldsymbol{y}, \tag{3.1}$$

where P_1 is the Lagrangian transition probability density for the displacement of a material particle.

Similarly the two-point concentration correlation has the form

$$\langle C(\boldsymbol{x}_1, t)\, C(\boldsymbol{x}_2, t)\rangle = \int P_2(\boldsymbol{x}_1, \boldsymbol{x}_2, t\,|\,\boldsymbol{y}_1, \boldsymbol{y}_2, s)\, S(\boldsymbol{y}_1)\, S(\boldsymbol{y}_2)\, \mathrm{d}^3\boldsymbol{y}_1\, \mathrm{d}^3\boldsymbol{y}_2$$

and, in particular, the second moment of concentration is

$$\langle C(\boldsymbol{x}, t)^2\rangle = \int P_2(\boldsymbol{x}, \boldsymbol{x}, t\,|\,\boldsymbol{y}_1, \boldsymbol{y}_2, s)\, S(\boldsymbol{y}_1)\, S(\boldsymbol{y}_2)\, \mathrm{d}^3\boldsymbol{y}_1\, \mathrm{d}^3\boldsymbol{y}_2. \tag{3.2}$$

Here P_2 is the Lagrangian transition probability density for the joint location of two material particles. The precise interpretation of (3.2) is that of a limit as $\boldsymbol{x}_1 \to \boldsymbol{x}_2$, where in practice a finite small separation is maintained but which is a smaller distance than that over which concentration statistics vary significantly. This interpretation is discussed in Durbin (1980) and Thomson (1987).

Clearly higher-order statistics require correspondingly higher-order joint particle statistics, but in this paper we shall only consider the particle-pair behaviour and consequently can only calculate the concentration variance. In particular, we cannot estimate the skewness of the concentration field since this would require a three-particle model.

3.2. *Infinite Péclet number*: *Thomson's* (1990) *model*

Molecular diffusion allows the material particles to shift between different fluid particles, which is a complicated process (but is modelled later rather simply, as in Sawford & Hunt 1986). When molecular diffusion is negligible, however, it is possible to associate material particles with Lagrangian fluid particles for all time, which is the level at which Thomson's model operates. Thomson's model gives the joint behaviour of fluid particle pairs. It does this by specifying a stochastic process for the instantaneous rate of change of the velocities of a pair of fluid particles, given their separation and velocities at some earlier instant. The physical process is approximately Markovian and has continuous trajectories and continuous velocity records (Sawford & Borgas 1994) and therefore is modelled by a Langevin equation for 'diffusion' in velocity phase space:

$$\mathrm{d}u_i = a_i(\boldsymbol{u}, \boldsymbol{x}, t)\, \mathrm{d}t + (C_0\bar{\epsilon})^{1/2}\, \mathrm{d}W_i, \tag{3.3}$$

where a_i is an unknown function and $\mathrm{d}W_i$ is white noise. As in Borgas & Sawford (1994*b*), the vectors are six-dimensional with the first three components describing particle one and the last three particle two. In homogeneous isotropic turbulence, the dependence of a_i reduces to dependence upon the particle velocities and upon the three-dimensional particle separation vector $\boldsymbol{\Delta}$. The constant C_0 is a universal number which describes the inertial-range Lagrangian velocity statistics. The drift vector a_i is only

partly understood in the context of such modelling: it must satisfy a well-mixed criterion (Thomson 1990) but is not determined uniquely by this condition; there are lesser constraints that are required for a strictly correct model (Borgas & Sawford 1994*b*). Generally, however, reasonable forms of a_i give acceptable results and Thomson's model is relatively simple and robust for many of the physical quantities of interest. We shall not here attempt to consider the general class of stochastic models. The main goal of this paper it to show that at least one two-particle stochastic model can reasonably account for at least one set of measured concentration fluctuations.

Fluid-particle displacements are determined by Thomson's model with the simple kinematic relation

$$\mathrm{d}x_i = u_i\,\mathrm{d}t, \tag{3.4}$$

again for six-dimensional vectors. This relation is straightforward, but is modified when we consider material–particle motions; then we use Thomson's well-mixed conditions to determine suitable additional forms.

The well-mixed criterion of Thomson (1987, 1990) ensures that a globally uniform source of tracer is not unmixed by the random motion of the turbulence. It is widely regarded as the most important constraint in Lagrangian particle stochastic models. It is most clearly obtained from the Eulerian stochastic formulation, which according to the Lagrangian modelling principles, is described by the Fokker–Planck equation for the Lagrangian transition p.d.f.,

$$\frac{\partial P_2}{\partial t} + u_i \frac{\partial P_2}{\partial x_i} = -\frac{\partial a_i P_2}{\partial u_i} + \tfrac{1}{2} C_0 \bar{\epsilon} \frac{\partial^2 P_2}{\partial u_i \partial u_i}, \tag{3.5}$$

where the displacements and velocities refer to fluid particles, i.e. we have not yet provided a model for the motions of material particles. The well-mixed criterion is developed by averaging the P_2 distribution over the initial state of fluid particles (according to the prevailing Eulerian distribution of fluid velocities at time s). Since this process yields the unbiased velocity distribution

$$P_E(\boldsymbol{u}, t \,|\, \boldsymbol{x}) = \int P_2(\boldsymbol{u}, \boldsymbol{x}, t \,|\, \boldsymbol{v}, \boldsymbol{y}, s)\, P_E(\boldsymbol{v}, s \,|\, \boldsymbol{y})\, \mathrm{d}^6\boldsymbol{v}\, \mathrm{d}^6\boldsymbol{y}, \tag{3.6}$$

the well-mixed condition is

$$\frac{\partial P_E}{\partial t} + u_i \frac{\partial P_E}{\partial x_i} = -\frac{\partial a_i P_E}{\partial u_i} + \tfrac{1}{2} C_0 \bar{\epsilon} \frac{\partial^2 P_E}{\partial u_i \partial u_i}. \tag{3.7}$$

Since we take P_E to be known, this equation represents a constraint on $\boldsymbol{a}$, but does not determine the drift term uniquely. In general, no known constraints do so. However, using a Gaussian distribution to approximate P_E it is possible to obtain simple forms for $\boldsymbol{a}$ (quadratic form in the velocity $\boldsymbol{u}$) which generate Lagrangian results which are reasonable. Thomson's drift term for

$$P_E = (2\pi)^{-3} \lambda^{-1/2} \exp\left(-\tfrac{1}{2}\lambda_{ij} u_i u_j\right) \quad (\lambda = \|\lambda_{ij}\|)$$

is given by

$$a_i = \tfrac{1}{2}\lambda_{jl} \frac{\partial \lambda_{il}^{-1}}{\partial t} u_j + \tfrac{1}{2}\lambda_{jl} \frac{\partial \lambda_{il}^{-1}}{\partial x_k} u_j u_k - \tfrac{1}{2} C_0 \bar{\epsilon} \lambda_{ij} u_j = \phi_i - \tfrac{1}{2} C_0 \bar{\epsilon} \lambda_{ij} u_j, \tag{3.8}$$

where $\langle u_i u_j \rangle = \lambda_{ij}^{-1}$ is the velocity covariance tensor which depends upon $\boldsymbol{\Delta}$, the spatial separation of sampling points. Furthermore, in isotropic turbulence this tensor depends on a single scalar function: the longitudinal correlation of velocity, $\sigma_u^2 f$, which

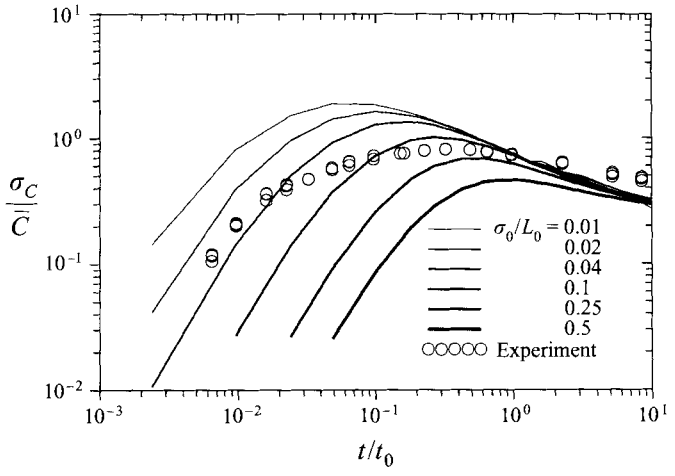

FIGURE 1. Normalized centreline concentration fluctuations for Thomson's inertial-range model. Each curve is for a different source size and the open circles show Sawford & Tivendale's (1992) experiments for which $\sigma_0/L_0 \sim 0.02$ and $m = 0.7$. The universal constant is given the value $C_0 = 6$.

depends on the scalar Δ, where $\Delta^2 = \Delta_i \Delta_i$. For self-similar decaying turbulence we use the parameterization

$$f(\Delta) = f\left(\frac{\Delta}{L(t)}\right) = 1 - \tfrac{1}{2}C\left(\frac{\Delta^2}{\Delta^2 + L(t)^2}\right)^{1/3}, \tag{3.9}$$

where C is Kolmogorov's constant and is approximately 2; this form has been used extensively in the past (Durbin 1980; Sawford & Hunt 1986; Thomson 1990; Borgas & Sawford 1994*b*) and explicitly includes inertial-range behaviour for the smallest resolved scales. Below (in §4) we modify $f(\Delta)$ to incorporate dissipation ranges as in Sawford & Hunt (1986).

Borgas & Sawford (1994*b*) have considered the problem of determining $\boldsymbol{a}$ in great detail, but in practical terms have found it difficult to improve greatly upon Thomson's model despite showing that in principle it has fundamental flaws. For the purposes of this paper, which is not necessarily to advocate a best model but rather to examine the possibility of explaining features of experiments, Thomson's model will be the basis of the work. The encouraging results that are given later justify this choice, but if the results had proven inexplicable with a model based on Thomson's form it would have been necessary to pursue other avenues.

Model (3.8) can be used to determine the standard deviation of concentration fluctuations (see §5 below) and the results for the centreline value are shown in figure 1. Also shown are the measurements of Sawford & Tivendale (1992). Clearly, the modelling has failed by some measures to describe many of the features of the experiments: the reasons why and the means to improve these models are our goals. Our hypothesis is that it is the neglect of molecular diffusion and of viscous dissipation ranges which is responsible for most of the differences. One straightforward approximation is that these small-scale effects may be accounted for simply with an effective source size many times the actual physical value. This is only partly true however, as a number of model predictions are shown in figure 1 for a sequence of ever larger source sizes, none of which adequately reflects the measured fluctuations for a broad range of times. Neither do alternative values of the uncertain universal constant C_0, here taken to be 6, remedy the modelling deficiencies. (Below we do allow for

Reynolds-number dependence of C_0 and also modify the form of the governing equations.) The main point of this section is that it is certainly necessary to modify Thomson's model in order to adequately explain the wind-tunnel measurements.

4. Two-particle stochastic models: material–particle model

The material–particle model that we develop (following Sawford & Hunt 1986) will be heavily based on Thomson's inertial-range model and, at the very least, will be forced to obey an appropriate well-mixed condition. In fact, this will constrain two drift terms: a_i in the equation for fluid-particle velocities and b_i in the equation for material-particle displacements (which will now also satisfy a Langevin equation). Of course, we continue to emphasize Markovian modelling, as this seems approximately correct for high-Reynolds-number turbulence, but allow dissipation ranges to enter the modelling in an *ad hoc* way by parameterizing viscous effects in the velocity structure functions. In particular, we do not alter the high-frequency structure of one-particle accelerations (as in Sawford 1991), which is altogether too complicated, and in any case partly compensated for since we fit the value of C_0 to mimic one-particle results. Two-particle accelerations derived from stochastic models are not physical even for inviscid models (Borgas & Sawford 1994*b*) and no attempt is made here to properly model the dissipation ranges when molecular effects are included. The principle constraint applied in this paper is Thomson's well-mixed condition and some simple two-to-one reductions of Borgas & Sawford (1994*b*).

The new model begins with the equation for material-particle displacements, which can be written similarly to above as

$$\mathrm{d}x_i = (u_i + b_i)\,\mathrm{d}t + (2\kappa)^{1/2}\,\mathrm{d}W'_i, \tag{4.1}$$

where u_i is the velocity of the fluid particle in which the material particle at present resides, b_i is a drift term as a consequence of the diffusion and is partly determined by the well-mixed condition and κ is the coefficient of molecular diffusivity (or thermal diffusivity). It is important to distinguish between fluid-particle velocity and material-particle velocity since the latter, according to the white noise $\mathrm{d}\boldsymbol{W}'$, does not exist. However, Eulerian velocity statistics are not altered by this distinction; only Lagrangian quantities are affected.

The choice of generalized material particle advection with $\boldsymbol{b}$ is simply a mathematical convenience (explained below) and is not strictly physical. In our case $\boldsymbol{b}$ is a function of the separation of two particles and each particle's velocity (see below) and it is proportional to κ, and therefore is 'small'. We shall also find that $\boldsymbol{b}$ vanishes in two-to-one reduction (Borgas & Sawford, 1994*b*) and is insignificant for longer dispersion times.

The companion equation of (4.1) is an equation for the fluid-particle velocity in which the material particle is found at each instant. This is potentially different from the equation for a labelled fluid particle (or pair of particles) which is the usual Lagrangian concept. Now we allow for different fluid particles to contribute to the velocity history where each fluid particle contributing to this history is marked at some instant by the presence of the material particle. Nevertheless, the process must be approximately Markovian, perhaps even more so than a pure fluid-particle process, and moreover remains continuous in the velocity phase space. Therefore, the equation that we use is just a Langevin equation (a diffusion process)

$$\mathrm{d}u_i = \tilde{a}_i(\boldsymbol{u}, \boldsymbol{x}, t)\,\mathrm{d}t + (\tilde{C}_0\bar{\epsilon})^{1/2}\,\mathrm{d}W_i,$$

where $\tilde{a}_i$ is an unknown function and $\mathrm{d}W_i$ is white noise. This equation is of course very similar to the previous equation for the velocity process, (3.3), but we formally allow the drift vectors to be different. Note that the interpretation also differs: this equation gives a stochastic estimate of the fluid-particle velocities 'seen' by the wandering material particles and not the Lagrangian velocities of labelled fluid particles. Consequently, the value of the coefficient of the white noise is allowed to differ from the non-diffusive case. This constant, $\tilde{C}_0$, is estimated in this paper by comparison with mean concentration statistics, but is otherwise unknown and is certainly allowed to differ from C_0.

The well-mixed condition applied to the joint material/fluid-particle process gives rise to the equation

$$\frac{\partial P_E}{\partial t}+\frac{\partial (u_i+b_i)\,P_E}{\partial x_i}=-\frac{\partial \tilde{a}_i\,P_E}{\partial u_i}+\tfrac{1}{2}\tilde{C}_0\,\bar{\epsilon}\,\frac{\partial^2 P_E}{\partial u_i\,\partial u_i}+\kappa\frac{\partial^2 P_E}{\partial x_i\,\partial x_i}, \tag{4.2}$$

where the Eulerian distribution of fluid-particle velocities, P_E, for given material-particle positions, is the same as the distribution for given sampling points. Thus we may choose as a solution a drift vector $\tilde{\boldsymbol{a}}$ essentially identical to Thomson's term. This partitioning of (4.2) leaves the condition

$$\frac{\partial b_i\,P_E}{\partial x_i}=\kappa\frac{\partial^2 P_E}{\partial x_i\,\partial x_i}$$

in order to satisfy the well-mixed constraint. A simple solution for b_i according to this condition is

$$b_i=\kappa\frac{\partial}{\partial x_i}\log P_E, \tag{4.3}$$

which is the model we shall use. An alternative choice with $\boldsymbol{b}=0$ requires that $\tilde{\boldsymbol{a}}$ be modified to account for the $\kappa\nabla^2 P_E$ term in (4.2). This requires at the very least cubic forms of $\tilde{\boldsymbol{a}}$ with respect to velocity and consequently very laborious determinations of unwieldy algebraic expressions for the drift term, severely reducing the efficiency of numerical computations. Our choice is to sacrifice the higher-order small-time integrity of the advection to produce as simple a model as possible with molecular effects included. Thus non-zero $\boldsymbol{b}$ is assumed.

Calculations with this model indicate that this choice is reasonable and no others will be considered. Note that if the molecular diffusivity is taken to be vanishingly small, then the time series for the velocity of (distinct) fluid particles, which have been sequentially marked by a material particle, should approach that along a fluid-particle trajectory. Therefore it is natural that Thomson's model should be the basis of the present model for the velocity process and that any deviations from it should vanish when $\kappa=0$.

To specify the model completely we need a $f(\Delta)$ parameterization which includes dissipation ranges (and possibly inertial ranges). The form we take is

$$f(\Delta)=1-\left(\frac{\Delta^2}{\alpha\eta^2+\Delta^2}\right)^{2/3}\left(\frac{\Delta^2}{\ell^2+\Delta^2}\right)^{1/3}. \tag{4.4}$$

Here η is Kolmogorov's microscale,

$$\eta=(\nu^3/\bar{\epsilon})^{1/4},$$

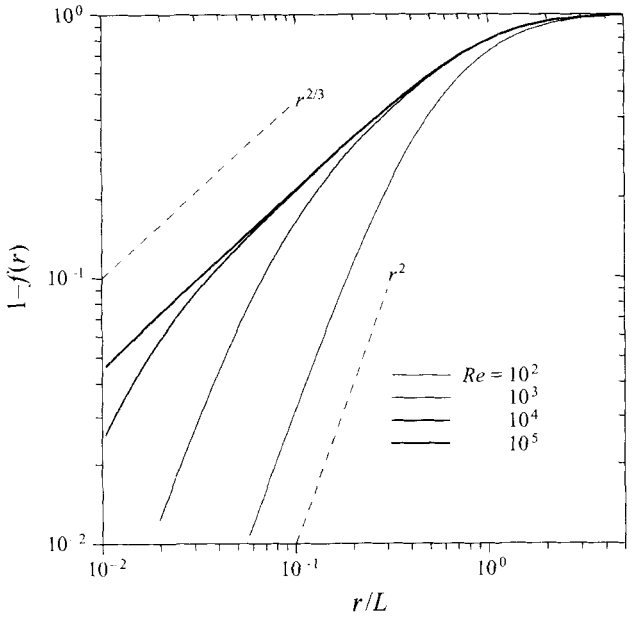

FIGURE 2. The parameterized velocity field longitudinal structure function, $1-f(r)$, shown for several Reynolds numbers. Only for very large Re is any inertial-range behaviour ($\frac{2}{3}$ power law) evident.

ℓ is determined by inertial-range properties, and α is a constant determined by the standard definitions. In the inertial range (for sufficiently large Re)

$$f \sim 1-\tfrac{1}{2}C\frac{(\bar{\epsilon}\Delta)^{2/3}}{\sigma_u^2} \sim 1-\tfrac{1}{2}C\left(\frac{\Delta}{L}\right)^{2/3} \sim 1-\left(\frac{\Delta}{\ell}\right)^{2/3};$$

thus as $C \approx 2$, $\ell \approx L$. Next consider the far dissipation range ($\Delta \ll \eta$), where

$$f \sim 1-\alpha^{-2/3}Re\left(\frac{\Delta}{L}\right)^2 \sim 1-\frac{1}{2}\left(\frac{\Delta}{\lambda}\right)^2,$$

the last by definition. The parameterization therefore requires that

$$\lambda = \frac{\alpha^{1/3}}{(2Re)^{1/2}}L,$$

which together with $Re_\lambda = \sigma_u \lambda/\nu = (15Re)^{1/2}$, gives

$$\alpha^{1/3} = \sqrt{30} \Rightarrow \alpha = 164.32. \tag{4.5}$$

This differs from Sawford & Hunt's (1986) parameterization ($\alpha = 42.6$), but their model was one-dimensional and as such has model-specific interpretations of representative quantities.

Figure 2 shows the form of $f(\Delta)$ for a different Re, clearly indicating a difficult-to-observe inertial range for the values of Re appropriate for wind-tunnel experiments. However, we elect to use a form that formally gives the inertial-range behaviour for sufficiently large Re because it is precisely this limit that interests us from the atmospheric perspective.

One of the reasons for favouring Thomson's (1990) model is that the two-particle model produces excellent one-particle statistics for velocity and displacement when a

single particle is considered independently of the other. This is despite explicit violation of this independence property in principle (Borgas & Sawford 1994*b*). In a practical sense, it is important that the one-particle behaviour is good because we intend to use these properties to select $\tilde{C}_0$. It is therefore encouraging to find that the new model is equally effective at modelling the one-particle dispersion of a material particle as was Thomson's model for the dispersion of a single fluid particle. Note that this is not equivalent to considering coincident particles, i.e. that the separation vanishes. Thomson's model strictly requires finite (inertial-range) separations at all times; despite our inclusion of viscous effects, neither can our model correctly represent the proper single-particle character as particles approach coincidence. We simply hope that the viscous effects we include impose the correct trend by damping the separation motions of particles which are already separated.

Coincidence of fluid particles is also a factor in considerations of incompressibility of the flow (Kaplan & Dinar 1988); for if particles are close enough for the local flow to be a simple shear flow, then in the limit of coincidence, the Jacobian of the Lagrangian transformation can be defined, which must be unity in each instantaneous realization of trajectory evolution for an incompressible flow. However, when the particles are constrained to be a finite distance apart, the Lagrangian incompressibility constraint cannot be applied in a single realization and incompressibility is trivially satisfied, as in the case of one-particle models. For separated trajectories we would actually need a three-particle model, where two of the three particles approached coincidence, in order to apply an incompressibility constraint for each realization of the triple trajectory evolution (where two of the trajectories are arbitrarily close to one another).

5. Concentration statistics

In this section calculations with the new model are shown to better account for the small-source-size experiments of Sawford & Tivendale (1992). These results instil confidence in the stochastic-equation approach since the degree of fitting is minimal and since the model is physically based (i.e. it is not just a fitted stochastic process). However, first (§5.1) the model is formulated in the reversed sense, i.e. for trajectories from the receptor back to the source because this is a more efficient way of dealing with the transport. Secondly, an approximation is introduced (§5.2) by explicitly partitioning the particle-pair displacements into centre-of-mass and separation coordinates, and assuming these components are independent. This approximation has been used extensively in the literature and keeps the statistical noise manageable for longer times. The remainder of the section (§5.3) gives the model results, and it is the most important part of the section.

5.1. *Reversed trajectories*

As in other studies it is convenient to consider dispersion modelling in the reversed sense where we model the paths from a given point (the concentration measurement point) at time t, to random initial points at time s. Only those trajectories that pass through the source initially will contribute to the accumulation of material at the measurement point. Thomson (1987, 1990) shows how to determine an appropriate well-mixed model for reversed trajectories by considering the backwards Kolmogorov equation:

$$\frac{\partial P_2}{\partial s}+(v_i+b_i)\frac{\partial P_2}{\partial y_i}=-\tilde{a}_i\frac{\partial P_2}{\partial v_i}-\tfrac{1}{2}\tilde{C}_0\,\overline{\epsilon}\frac{\partial^2 P_2}{\partial v_i\,\partial v_i}-\kappa\frac{\partial^2 P_2}{\partial y_i\,\partial y_i},$$

where $P_2 = P_2(\boldsymbol{u}, \boldsymbol{x}, t \mid \boldsymbol{v}, \boldsymbol{y}, s)$ is the forward transition probability density for displacements and velocities of two material particles, i.e. $t > s$. The coefficients $\boldsymbol{a}$ and $\boldsymbol{b}$ are the functions used in the forward model, (3.8) and (4.3), except that they are evaluated with the independent variables at time s, $\boldsymbol{y}$ and $\boldsymbol{v}$ respectively.

Using Thomson's (1987) result that

$$P_2(\boldsymbol{u}, \boldsymbol{x}, t \mid \boldsymbol{v}, \boldsymbol{y}, s)\, P_E(\boldsymbol{v}; \boldsymbol{y}, s) = P_2(\boldsymbol{v}, \boldsymbol{y}, s \mid \boldsymbol{u}, \boldsymbol{x}, t)\, P_E(\boldsymbol{u}; \boldsymbol{x}, t),$$

which is still valid when molecular diffusion effects are included, and with the changed independent variables

$$t' = -s, \quad \boldsymbol{u}' = -\boldsymbol{v}, \quad \boldsymbol{x}' = \boldsymbol{y},$$

then the reversed model is identical in appearance to the forward model except for primes on the independent variables. Thus the corresponding Langevin equation (equivalent to (3.3) and (4.1) in primed variables) can be used to develop the reversed-trajectory statistics.

In the reversed problem, however, the parameters σ_u^2 and $\bar{\epsilon}$ grow with time t', and concurrently the lengthscale L becomes smaller. Suppose that we have made all variables non-dimensional with respect to source parameters (at time $t = 0$). We are interested in the statistics at time $t = Tt_0$ $(T > 0)$, which is equivalent to $x = Tx_0$ downstream in the stationary-frame wind-tunnel context. The parameters in reversed time t' (made dimensionless with t_0), where $t' = 0$ corresponds to $t = Tt_0$ and $t' = T$ corresponds to $t = 0$, are

$$\sigma_u^2 = (1 + T - t')^{-2m}, \quad L = (1 + T - t')^{1-m},$$

which may be used in a time-dependent transformation of the problem. We now transform velocities and length to variables proportional to $\sigma_u(t')$ and $L(t')$ respectively, and use a transformed time τ according to

$$\frac{\mathrm{d}\tau}{\mathrm{d}t'} = \frac{\sigma_u}{L} \Rightarrow \tau = -\log\left(1 - \frac{t'}{1+T}\right).$$

The transformed problem is effectively stationary when $m = 0.5$ (when dissipation ranges are included) or for any m in the case of a strictly inertial-range model. Thus in this case we can calculate an ensemble of transformed particle-pair trajectories beginning (i.e. ending in real forward time) with a negligibly small separation, for a fixed τ-interval. Then each lag less than τ can be used as another effective final time for calculating concentration statistics, i.e. this same ensemble can be used for calculating the full time development of the concentration fluctuations.

In contrast, when $m \neq 0.5$ and with dissipative ranges, which is the case most relevant here, we must compute a new ensemble of trajectories for each final time. This is because, although the velocity variance is constant in the transformed problem, the dissipation lengthscale of the spatial correlation of velocities changes with transformed time. Thus the ensemble of trajectories for a fixed final time τ_1 cannot be transformed to give the equivalent ensemble for a shorter elapsed time τ_2. In fact, when $m \neq 0.5$ it may be more efficient computationally to pursue forward-time integration, but this is not a critical issue in this study.

5.2. *Separation/centre-of-mass approximation and scaling*

The Monte-Carlo numerical solution of the stochastic model employed here necessarily uses a finite number of realizations and as a consequence there are difficulties in resolving concentration fluctuations at large times. The reversed trajectories have in

this instance wandered far from the origin and limited numbers intercept the source. Thus the concentration statistics are progressively degraded. One method of improving this performance is to use an approximation due to Sawford (1983) which has been used in other relative dispersion studies. In particular, Thomson (1990) has shown its utility for the stochastic-model relative dispersion problem and likewise we have checked and verified its validity for the present model.

The dispersion of material is now estimated semi-analytically by approximating P_2 (for reversed trajectories) by

$$P_2(\boldsymbol{x}_0, \boldsymbol{\Delta}_0, s \mid \boldsymbol{x}, \boldsymbol{\Delta}, t) \approx G(z_0, s \mid z, t)\, P(\boldsymbol{\Delta}_0, s \mid \boldsymbol{\Delta}, t), \tag{5.1}$$

where G represents the Gaussian form and P is unknown. The variables in (5.1) are the centre of mass and material-pair separation:

$$z = \frac{(x' + x)}{\sqrt{2}}, \quad \boldsymbol{\Delta} = \boldsymbol{x}' - \boldsymbol{x}$$

respectively; the approximation is an independence hypothesis for these uncorrelated variables, together with the further assumption of Gaussian displacements of the centre of mass with (reverse) variance $\sigma_Z^2(t)$. Furthermore, for an instantaneous Gaussian source of mass S_M (in total when $M = 0$; per unit length when $M = 1$; per unit area when $M = 2$) spread over lengthscale σ_0, it follows that

$$\langle C^2(\boldsymbol{x}) \rangle = S_M^2\, G_M(\sqrt{2}\boldsymbol{x}; \sigma_Z^2 + \sigma_0^2) \int P(\boldsymbol{\Delta}_0, s)\, G_M\left(\frac{1}{\sqrt{2}}\boldsymbol{\Delta}_0; \sigma_0^2\right) \mathrm{d}^3\boldsymbol{\Delta}_0, \tag{5.2}$$

where M denotes the topology of the source ($M = 0$ for a point source, $M = 1$ for a line source and $M = 2$ for an area source); and, for example,

$$G_2(x; \sigma^2) = \frac{1}{(2\pi)^{1/2}\sigma} \exp\left(-\frac{1}{2}\frac{x^2}{\sigma^2}\right),$$

where x measures distance normal to the centreplane of the area source.

Thus the numerical task requires us to find σ_Z^2, and, for N realizations of initial particle separation $\boldsymbol{\Delta}_i$, to compute the average

$$c^2 = \frac{1}{N}\sum_{i=1}^{N} G_M\left(\frac{1}{\sqrt{2}}\boldsymbol{\Delta}_i; \sigma_0^2\right)$$

so that

$$\langle C^2(\boldsymbol{x}) \rangle = S_M^2\, c^2 G_M(\sqrt{2}\boldsymbol{x}; \sigma_Z^2 + \sigma_0^2).$$

The cross-stream profile of the concentration fluctuations, σ_C, defined as

$$\sigma_C^2(\boldsymbol{x}) = \langle C^2(\boldsymbol{x}) \rangle - \langle C(\boldsymbol{x}) \rangle^2,$$

is, according to the approximations for an area source ($M = 2$),

$$\sigma_C^2 = S_2^2(c^2 G_2(\sqrt{2}\boldsymbol{x}; \sigma_Z^2 + \sigma_0^2) - G_2(\boldsymbol{x}; \sigma_1^2 + \sigma_0^2)^2), \tag{5.3}$$

where σ_1^2 is the one-particle dispersion and the subscription on G denotes the dimensionality of the source (2 ≡ area source). Thomson normalizes his profiles with the value of the centreplane fluctuation:

$$\sigma_C^2(0) = \frac{S_2^2}{2\pi}\left(\frac{(2\pi)^{1/2}c^2}{(\sigma_Z^2 + \sigma_0^2)^{1/2}} - \frac{1}{\sigma_1^2 + \sigma_0^2}\right).$$

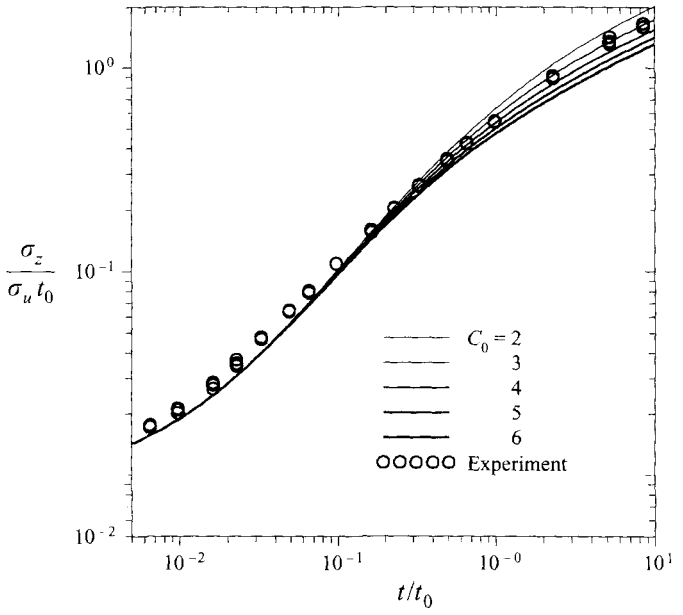

FIGURE 3. One-particle dispersion (from mean concentration profiles). Experiments (circles) and modelled results (curves) for different $\tilde{C}_0$ values. Non-self-similar decay, $m = 0.7$, is best fit by $\tilde{C}_0 = 3$. $\sigma_0/L_0 = 0.01$.

If we let $x = (\sigma_1^2 + \sigma_0^2)^{1/2} X$ be the normal distance from the source centreplane and $\varsigma^2 = (\sigma_Z^2 + \sigma_0^2)/(\sigma_1^2 + \sigma_0^2)$, then fluctuation profiles normal to the centreplane are given by

$$\frac{\sigma_C^2}{\sigma_C^2(0)} = \frac{[2\pi(\sigma_1^2+\sigma_0^2)^{1/2}\varsigma^{-1}c^2 \exp(-\varsigma^{-2}X^2) - \exp(-X^2)}{[2\pi(\sigma_1^2+\sigma_0^2)]^{1/2}\varsigma^{-1}c^2 - 1}.$$

Line-source or point-source approximations can be found in a similar way.

5.3. *Results*

Before any meaningful wind-tunnel comparisons can be made the constant $\tilde{C}_0$ must be estimated. Here we choose this 'universal' constant so that the measured mean-concentration profiles are modelled correctly (our aim is to predict concentration fluctuations about this mean). Thomson (1990) gives the necessary results, (2.7), for one-particle dispersion (hence mean concentrations) for the case of self-similar decaying turbulence considered here. It is straightforward, by simple addition, to include the effects of molecular diffusion. These merely alter the small-time results and indeed improve the correspondence, but the structure of longer-time dispersion is influenced mainly by m and $\tilde{C}_0$.

Figure 3 shows the comparison of the one-particle dispersion measurements with theory, i.e. (2.7) combined with additive molecular effects (because of two-to-one reduction, this is practically equivalent to our stochastic equation results); the vertical concentration profiles are very nearly Gaussian, with downstream spread given in figure 3. The choice $\tilde{C}_0 = 3$ provides the best fit in this case ($m = 0.7$), but it should be noted that this value is sensitive to m (m is an exponent so absolute differences tend to be amplified exponentially).

Figure 4 is similar to figure 3, but shows the source-size dependence for $\tilde{C}_0 = 3$. Evidently a value of $\sigma_0 \approx 0.01 L_0$ is meaningful as far as the experimental mean

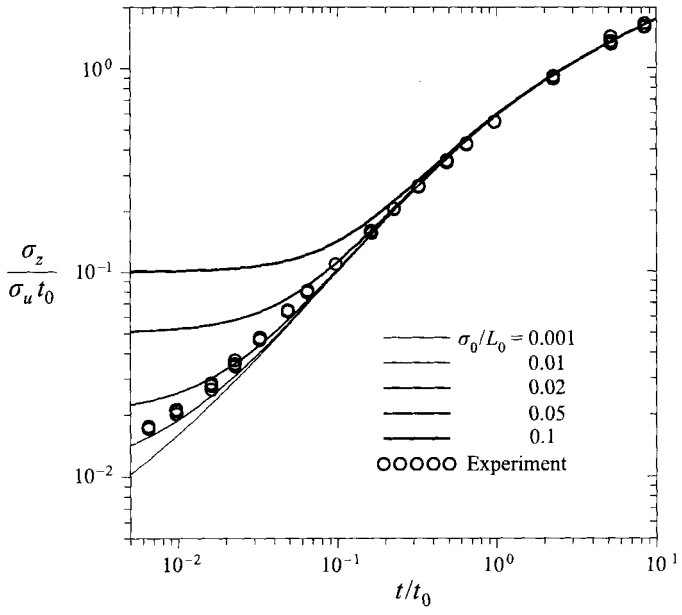

FIGURE 4. As for figure 3, but varying the source size parameter, σ_0, with fixed $\tilde{C}_0 = 3$.

concentrations are concerned. Thus σ_0 as estimated directly from the known diameter of the heated-wire source and as estimated from the one-particle dispersion are consistent.

The Péclet number for these two figures is $Pe = 60$, but this choice affects (along with σ_0) only the small to moderate scales of dispersion. $\tilde{C}_0$ is determined (for each m) by the larger-scale dispersion. Note that there is some evidence that a smaller Pe would better fit the data at smaller times; this would raise the curves slightly for the initial development and potentially allows a better fit than simply adjusting σ_0.

Anand & Pope (1985) find $\tilde{C}_0 = 2.1$ in an analogous procedure, but based on different wind-tunnel data ($m = 0.65$). In fact, the present data support a contradictory trend for if we take $m = 0.5$ the data are best fit by the theory when $\tilde{C}_0 = 6$. The fact that $\tilde{C}_0$ is apparently not universal is not a stumbling point here: the universal character is only attained at much larger Reynolds number. In our model $\tilde{C}_0$ is assumed to implicitly account for viscous timescales in the acceleration decorrelation, which are not modelled explicitly as in Sawford (1991). The last reference gives an estimate of the asymptotic limit of $\tilde{C}_0$ between 7 and 8 for large Re, but with values of $\tilde{C}_0$ around 3 appropriate for low Re, so the present estimate is not altogether unreasonable.

The model is now fully specified with no further parameters to be set. Calculations for $m = 0.5$ are shown in figure 5 for the normalized fluctuation on the centreline as a function of elapsed time (i.e. downstream distance). Because our definition for the length scale of the turbulence, L, depends on m, the appropriate Reynolds number for the self-similar case is $Re = 200$. A number of effective source sizes are used in the calculations, spanning the spectrum of relevant physical dimensions. Also shown are the experimental data. Evidently, there is a marked improvement from the inertial-range model even with an inappropriate value of m. The modifications for molecular effects clearly ensure that the peak fluctuations are better represented than in an inertial-range model for small source sizes (although there is still an over-prediction) and the small-time behaviour is much better. Turning to the $m = 0.7$ results in figure

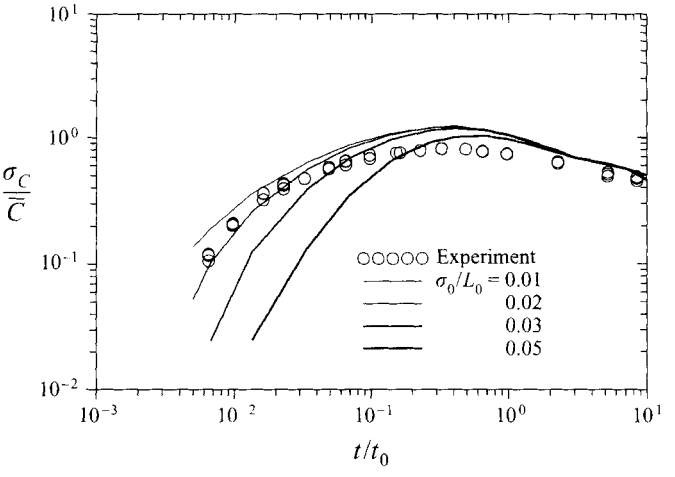

FIGURE 5. Normalized centreline concentration fluctuations for the material-particle model for self-similar decaying turbulence. Each curve is for a different source size and the open circles show Sawford & Tivendale's (1992) experiments. Source parameters are $Re = 200$, $Pe = 90$. We use $\tilde{C}_0 = 6$ for $m = 0.5$.

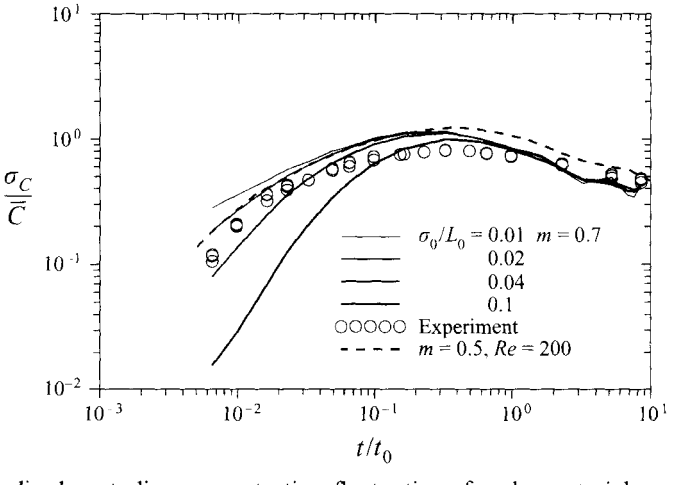

FIGURE 6. Normalized centreline concentration fluctuations for the material-particle model. Each curve in the figure is for a different source size and the open circles show Sawford & Tivendale's (1992) experiments. Source parameters are $Re = 144$, $Pe = 62$. We use $\tilde{C} = 3$ for $m = 0.7$. The self-similar case from figure 5 with $\sigma_0/L_0 = 0.01$ is also shown.

6 we find further, though slight, improvements. There is still a persistent over-prediction, but generally a remarkably similar shape compared to the measured distribution of fluctuations. There are indications of a slightly faster fall-off for larger times, and comparison with the $m = 0.5$ results suggest that an immediate value of m would better mimic the fluctuations. Unfortunately, statistical uncertainties develop towards the end of the simulation so that while a trend towards a constant $\sigma_C/\bar{C}$ is developing ($\sigma_C/\bar{C} \sim 0.3$), the asymptotic status remains uncertain.

Further encouraging results are evident in figure 7 which shows the comparison for the lateral distribution of fluctuations, normalized by the centreline fluctuation. Each curve in this figure corresponds to a different elapsed time (downstream location) and the bimodal–unimodal–bimodal transition is evident, although close to the source the

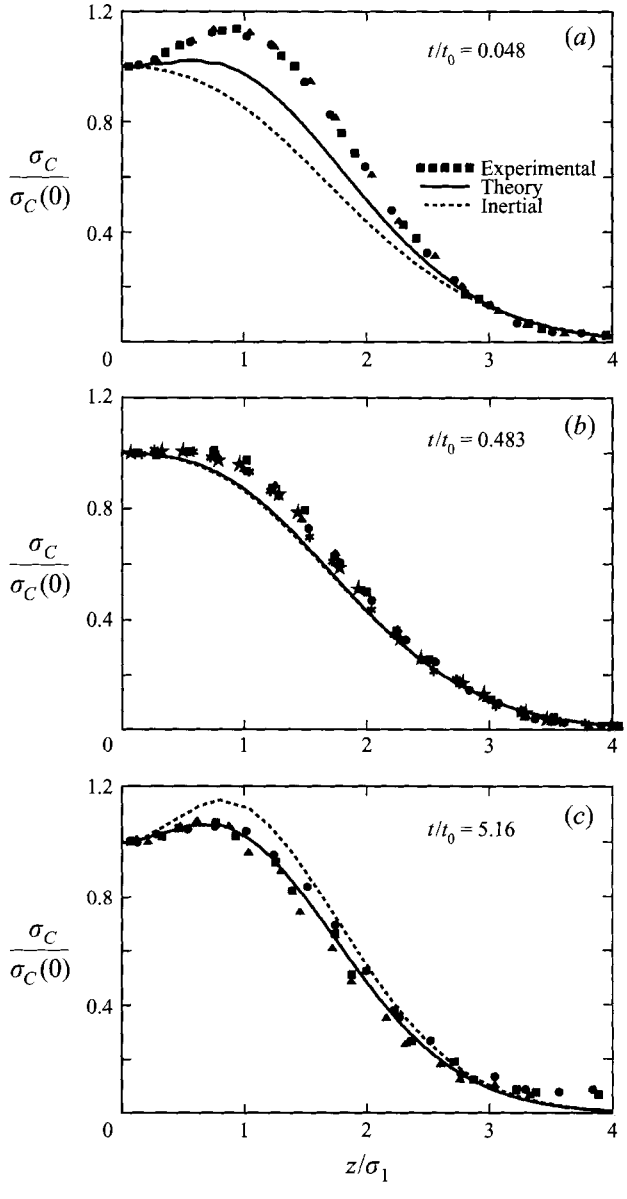

FIGURE 7. Lateral profiles of normalized fluctuations at three different times (downstream locations). Symbols give experimental values and the curves are from the material-particle model: $m = 0.7$, $Re = 144$ and $Pe = 62$. (*a*) A (weakly) bimodal distribution close to the source; (*b*) for the intermediate time, it is unimodal; and finally, farthest from the source, (*c*), it is bimodal. $\sigma_0/L_0 = 0.02$. The profiles for the inertial-range model are shown as dashed curves.

profile of $\langle C^2 \rangle$ is too narrow and the near-source distribution of σ_C is nearly unimodal. Note this structure also occurs in the inertial-range modelling, and the quantitative fit is also reasonable. This is because the normalization of the lateral intensities relative to the centreline intensity is quite forgiving in this instance.

We consider next the results for a hypothetical point source in the wind tunnel. Our temporal-transformation approximation treats this as an instantaneous line source laid along the x-axis which subsequently mixes radially outward in a cylindrical fashion.

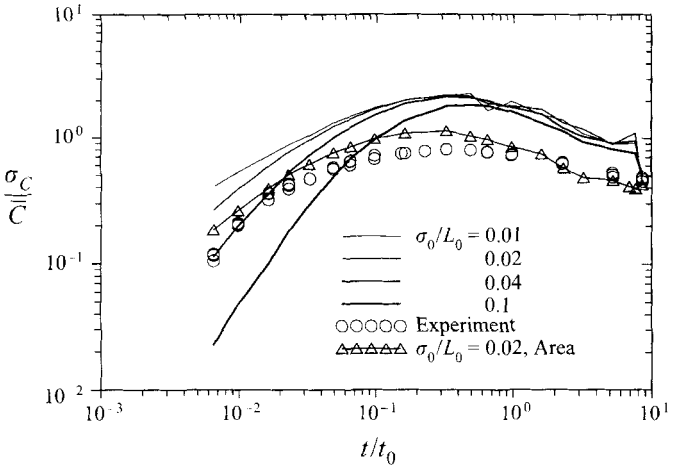

FIGURE 8. As for figure 6, but for a hypothetical wind-tunnel point source (i.e. instantaneous line source along the x-axis). No experimental data are shown for line sources, but the instantaneous area source (wind-tunnel line source) results are shown as open triangles (for $\sigma_0/L_0 = 0.02$).

The already fully parameterized model is used. The results (figure 8) show an expected increase in the level of fluctuations, but overall a similar shaped set of curves as for the wind-tunnel line source (which is modelled as an instantaneous area source). However, there appear to be qualitative differences for the radial (as opposed to vertical) profiles of the fluctuations, which are shown in figure 9 to lack significant bimodality. There are limited data for this source geometry (Gad-el-Hak & Morton 1979; Nakamura, Sakai & Miyata 1987). These data are not inconsistent with our results: the most comprehensive of them (Nakamura *et al.* 1987) are given for $t/t_0 > 8$ and show the fluctuations still rising (with intensities between 1 and 2) as a function of time (downstream distance). This can be understood in the context of the present model because the Reynolds numbers for these water-tunnel experiments are quite low, but the Prandtl number is enormous: $\sim 10^4$. Thus the main effect is of particles remaining close together under the influence of 'viscous forces' and this same effect is responsible for the 'overshoot' of intensities relative to inertial-range model predictions.

The over-prediction of intensities with the incorporation of molecular effects is the consequence of two competing effects: molecular diffusion acts to reduce the intensities, while viscous effects act to keep particles together and increase the intensities. In the absence of molecular diffusion, coincident particles can never separate and the intensities grow (Durbin, 1980; Sawford & Hunt 1986). In our model, and for the parameter ranges considered, the dominant effects are: first, the small-time behaviour is dominated by molecular diffusivity and there are no Re effects; second, the medium-time behaviour is dominated by the viscous resistance to particle-pair separation, thus the intensities overshoot the infinite Re results. Ultimately, we expect the long-time results to converge (since particle pairs will always separate and decorrelate eventually), but our numerical results are not statistically reliable enough to be useful in this limit.

For our model results, at least as far as the calculations appear statistically reliable, there are persistently higher intensities for the point-source results (Kaplan & Dinar (1988) noticed similar source-size dependence in their model for concentration-fluctuation intensities). As explained by Thomson (1990) these curves can converge only to zero as the material 'forgets' its initial state, but this is apparently at longer

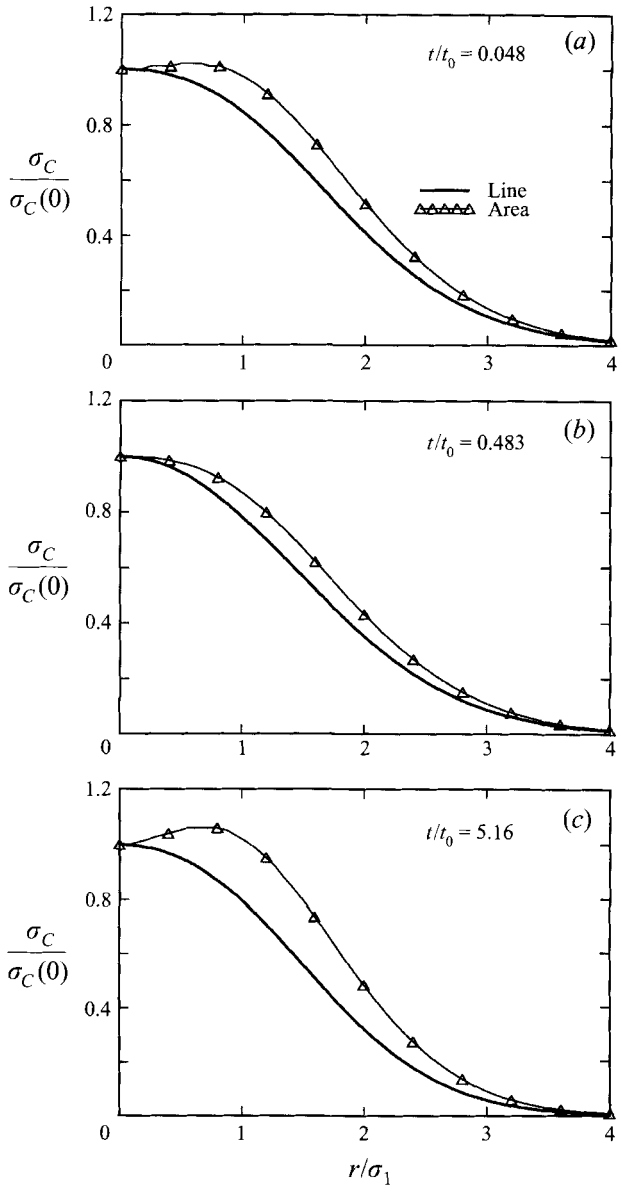

FIGURE 9. As for figure 7, but for a hypothetical wind-tunnel point source for $\sigma_0/L_0 = 0.02$ (i.e. instantaneous line source along the x-axis). No experimental data are shown. In this case the abscissa is a radial coordinate measured from the axis corresponding to the initial instantaneous source axis. The curve with open triangles corresponds to the theoretical curves in figure 7 (area-source results).

times (further downstream) than for which our model is reliable. It is not possible to decide whether or not the long-time asymptotic intensity of fluctuations is zero with our model. However, it is remarkable how slow the line-source results 'decay' relative to the area-source results; again, it is primarily the 'viscous overshoot' that is responsible for this effect.

Figure 10 shows a comparison of the new intensities with those from figure 1, i.e. using a purely inertial-range model. This figure shows that for large source sizes the molecular effects are less important but with a tendency for the inertial-range model to

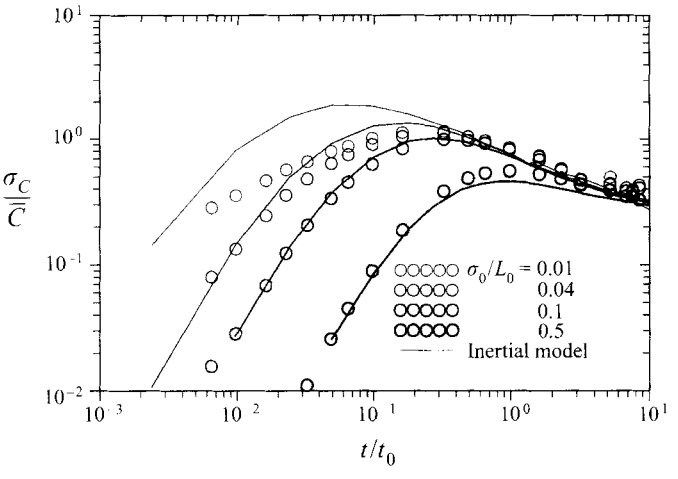

FIGURE 10. A comparison of figures 1 and 6 showing the source-size dependence for an inertial-range model (lines) and for a model with molecular effects (circles) respectively. The appropriate curves are better matched for larger σ_0.

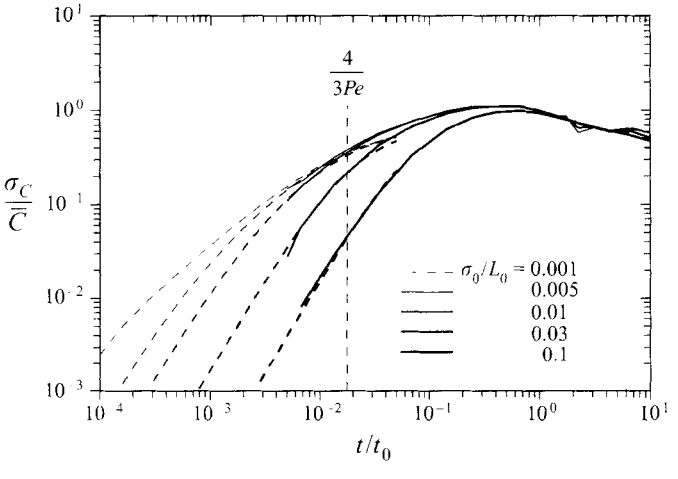

FIGURE 11. Small-time asymptotic expansion for the centreline intensity of fluctuations matched to the numerical results (for $m = 0.5$, $Re = 150$, $Pe = 75$) for a number of initial source sizes. The vertical dashed line shows the upper bound for the expected validity of the asymptotic results. $\tilde{C}_0 = 6$.

under-predict at large times, which is a little unexpected. This behaviour needs careful interpretation because the value of C_0 and $\tilde{C}_0$ differ (by a factor of 2) in the two instances. If C_0 were taken as 3 in the inertial-range model then the effect is to lower the long-time results of figure 1; thus the over-prediction of the molecular-effects model is enhanced.

The small-time behaviour, clearly better described by the new model, is shown in figure 11 together with a simple asymptotic development derived in the following section (§6). The good description of the small-time behaviour depends mainly on the leading-order effect of molecular diffusivity and of the Eulerian velocity statistics and thus is not a reliable indication that the present model of the Lagrangian characteristics

of the turbulence is good. However, the flatter shape of the curves and the fall-off trend for the large times are features dominated by the Lagrangian structure, i.e. when the simple molecular diffusion effects are less important, thus the general improvement of the predictions supports the Lagrangian model not just the added influence of molecular diffusion at small times.

At present there are no particularly useful asymptotic results in the large-time limit although Thomson (1990) has given some arguments related to the ultimate structure of the fluctuations. The present results, in particular the gross change in the shape of the centreline fluctuations, even for moderately long elapsed dispersion times, indicate that the effects of molecular diffusivity and particularly viscosity persist for quite significant times and that for the times considered to date it is not possible to ignore the dissipative effects. This represents a complication in any attempt to construct a long-time asymptotic theory.

The computations reported in this paper are quite expensive. A Cray Y-MP was used for most runs, some of which required 3 h of CPU simply to compute a single time point on figures 5 or 6 for the later dispersion times. Ironically, it is the low-Re cases which are most demanding. This is because the particles start close together and separate very slowly if the viscous effects are strong. The timescales resolved by the model are very short when the separation is small (an adaptive time step is used). Thus an enormous number of steps is required to separate the particles. In the inertial range (for high Re) the separation is very rapid. The other computational complication is statistical noise which becomes ever more significant as time increases. For short times the order of 2×10^4 pairs of particles gives reasonable statistics. For the longest of times as many as 5×10^4 gives no guarantee of good results but this number is adequate and is used for most purposes. Finally, we note that for low Re, there were occasional floating-point numerical problems for initial separations that are too small. Strictly speaking, for our model (4.2) and (4.3), which has unphysical singular forms for local fluid-particle acceleration as the separation Δ vanishes, requires that the separation not be much smaller than the Kolmogorov microscale η. For large enough initial separation, say 0.1η, there were no persistent problems. For large enough Re, it was found that no restrictions were necessary.

6. Saffman's results and asymptotic behaviour

Saffman (1960) considers the development of the displacement probability distribution for a material particle. His analysis is local in time and space and expands the velocity field in the neighbourhood of the particle with a Taylor series. A local solution of the advection–diffusion equation is solved in the approximation that diffusion dominates (i.e. for very short times) and for a single δ-function initial condition. He develops a small-time expansion for the velocity autocorrelation and can determine the mean-square dispersion accordingly. The results are

$$\langle x^2 \rangle = 3\sigma_1^2 = 6\kappa t + 3\sigma_u^2 t^2 - \tfrac{1}{3}\kappa t(t/t_\eta)^2 + O(t^4) \tag{6.1}$$

for the dispersion from a point source at the origin, $\langle x^2 \rangle$, and

$$\langle \Delta^2 \rangle = 6\sigma_\Delta^2 = 12\kappa t + \tfrac{4}{3}\kappa t(t/t_\eta)^2 + O(t^4) \tag{6.2}$$

for the spread about the centre of mass. These two expansions are valid only for times much smaller than t_η and therefore have limited use.

The stochastic model we use has definite flaws in terms of its microscale structure: first, because of the presence of the well-mixed term $\boldsymbol{b}$; secondly for its singular

representation of fluid-particle accelerations for vanishingly small separations; and thirdly, because of the white noise 'infinite' accelerations. In reality, fluid-particle accelerations are finite and scale as $(\bar{\epsilon}/t_\eta)^{1/2}$. The net result is that expansions for the stochastic model equivalent to (6.1) and (6.2) fail at third and second order in t respectively. The error due to $\boldsymbol{b}$ is in principle the most serious, but in practice is found to be rather weak both because the molecular diffusion is always considered a weak perturbative effect and also because two-to-one reductions ensure that $\boldsymbol{b}$ vanishes in the mean. The error due to white-noise accelerations is similarly not practically significant. The white-noise approximation of course represents a cumulative change in velocity increments over many microscale timescales and clearly any expansion based on smallness of time within the microscales is in error. However, it is almost never expected that models for such short time will be useful and instead we have chosen to provide a model for arbitrarily long-time evolutions, where the 'inertial-range' cumulative increments are modelled but with molecular modifications also included in a reasonable way. Thus when we consider the small-time behaviour we should concern ourselves with times small compared with the large scales, but larger than the microscales.

The small-time dispersion results are evidently dominated by molecular diffusion effects. An estimate of the fluctuations in this case comes from small-time approximation of (5.3), and with a small-Δ expansion giving c^2,

$$\frac{\sigma_C^2}{\bar{C}^2} = \frac{\sigma_1^2+\sigma_0^2}{(\sigma_1^2+\sigma_0^2+\rho\sigma_1^2)^{1/2}(\sigma_1^2+\sigma_0^2-\rho\sigma_1^2)^{1/2}} - 1 \approx \frac{1}{2}\left(\frac{\rho\sigma_1^2}{\sigma_1^2+\sigma_0^2}\right)^2$$

with the definition (of ρ) that $\sigma_\Delta^2 = \sigma_1^2(1-\rho)$. For small times greater than t_0

$$\rho \sim \tfrac{1}{2} Pe\, t \quad \text{and} \quad \sigma_1^2 \sim 2Pe^{-1}t + t^2.$$

These approximations are not significantly affected by Saffman's higher-order corrections nor by the singular terms in the stochastic model; as $\Delta \to 0$, such terms tend to have local effects for times much shorter than t_η and they do not significantly affect (6.1) and (6.2). Thus a good representation of the small-time behaviour is given by

$$\frac{\sigma_C^2}{\bar{C}^2} = \tfrac{1}{8}(Pe\, t)^2\left(\frac{2t+Pe\, t^2}{2t+Pe\, t^2+Pe\, \sigma_0^2}\right)^2, \tag{6.3}$$

which gives t^2 asymptotic behaviour and, for $2Pe^{-1}t \ll \sigma_0^2$, the initial behaviour

$$\frac{\sigma_C^2}{\bar{C}^2} = \frac{1}{8}\left(\frac{t}{\sigma_0}\right)^4.$$

From the comparison shown in figure 11 these results clearly describe the early behaviour of concentration fluctuations, and demonstrate that the small-time defects of the model are not practically important.

7. Large-Reynolds-number limit

The additional effects of molecular diffusion and viscous subranges appear to reconcile anomalous features of Thomson's (1990) Lagrangian stochastic model predictions with measurements of concentration fluctuations. Thus there is support for the idea that Thomson's model captures the underlying inertial-range structure of

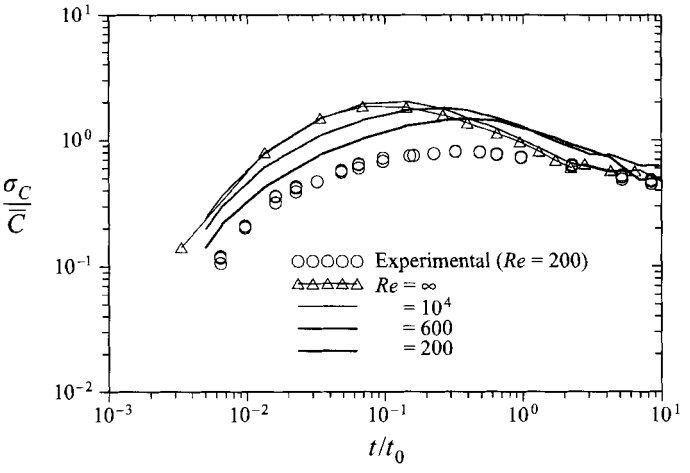

FIGURE 12. Normalized centreline concentration fluctuations for the material-particle model in self-similar decaying turbulence ($m = \frac{1}{2}$). The curves are for a sequence of increasing Re ($\tilde{C}_0 = 6 \,\forall\, Re$). The instantaneous area source size is $\sigma_0/L_0 = 0.01$ and the Prandtl number is $\frac{3}{4}$. Thomson's inertial-range result is shown as a curve with open triangles.

turbulent motions relevant for relative dispersion. This model derives from theoretical scaling properties in very large-Reynolds-number flows, but can apparently be modified for lower-Re flows by the present methods. It is of interest to observe the development of the large-Reynolds-number solution from the present model by performing calculations for a sequence of ever higher Pe and Re. To do this it must be understood that $\tilde{C}_0$ is a parameter in the finite-Péclet-number theory and approaches an uncertain limiting value in the limit $Re \to \infty$. It is the determination of this constant which is perhaps the most crucial element of modern Lagrangian dispersion theories for the atmosphere. However, for the present we shall consider (hypothetically) decaying turbulence with $m = 0.5$. For $\tilde{C}_0 = 6$ this gives realistic mean concentrations and intensities (see figure 5) when $Re = 200$. For infinite Reynolds numbers, a rough consensus also has $\tilde{C}_0 = 6$ (Sawford 1991; Rodean 1991); thus we shall suppose $\tilde{C}_0 = C_0 = 6 \,\forall\, Re$ for the examination of Re dependence when $m = 0.5$. Comparisons for different m may require that $\tilde{C}_0$ is Re dependent. For example, for low Re and $m = 0.7$, comparisons with the wind-tunnel data set used in this paper suggest that $\tilde{C}_0 = 3$. Similarly for stationary turbulence ($m = 0$)

$$\tilde{C}_0 = C_0 - 600/Re,$$

is a rough fit of Sawford's (1991) 'bulk' parameterizations from a one-particle model. However, since we are conducting a hypothetical 'thought' experiment to examine the approach to the infinite-Re limit, and are not necessarily restricting ourselves to a particular data set at low (Re say), then almost any kind of Re dependence in $\tilde{C}_0$ could be prescribed. We shall only consider the simplest.

For ease of computations we use $m = 0.5$ and $Pe = \frac{3}{4}Re$, so the results are not meant to have explicit bearing on the wind-tunnel measurements. Figure 12 then shows the approach of the concentration fluctuations to the levels predicted by Thomson's inertial-range-based model for an instantaneous area source. Reasonable convergence occurs for $Re \approx 10^4$. The small-scales are evidently most dependent upon dissipative effects, and for intermediate times (many t_η and at least several t_0) the lower-Re curves overshoot the $Re = \infty$ case giving larger intensities.

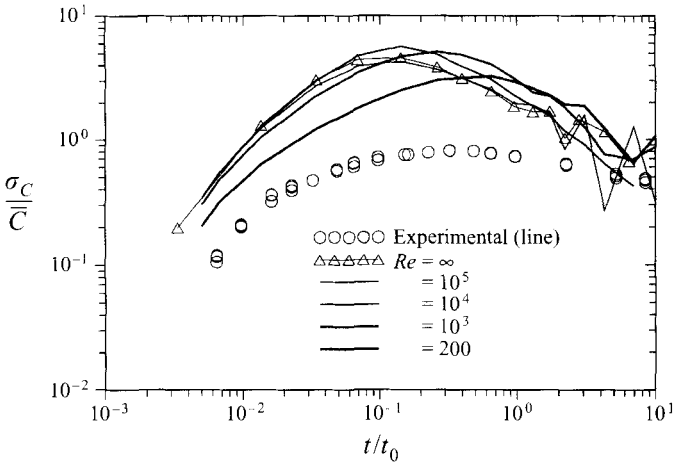

FIGURE 13. As for figure 12, but corresponding to a hypothetical wind-tunnel point source (i.e. an instantaneous line source along the x-axis) and for a different set of Reynolds numbers. Convergence to $Re = \infty$ is slower than in figure 12.

Figure 13 displays results appropriate for the instantaneous line source (in the transformed problem) for an increasing sequence of Re. The change of source geometry (equivalent to a continuous point source in the wind tunnel) has altered the convergence characteristics and a much larger Reynolds number, $Re \sim 10^5$, is required for the same agreement. Lower-Re results typically over-predict the concentration fluctuation: even for $Re = 10^4$, the value can be too large by as much as 30% for significant lengths of time. Overall there is an expected higher level of fluctuations for the line source for small to moderate times. For long times (i.e. far downstream) and large enough Re, the fluctuations decay but it is not possible to determine from the model results whether the asymptotic state is for zero intensities, i.e. converged line and area source results.

Naturally occurring flows in the atmosphere typically have $Re \geqslant 10^4$, therefore Thomson's (or some other) inertial-range model could be used in this case. If the sources have lengthscales smaller than η, then some effective source size must be used, but then the near-field results will be in error. However, it is unlikely that practical applications will need such small lengthscale definition.

These results indicate that the dispersion process in the atmosphere is dominated by inertial-range processes rather than by viscous or molecular-diffusion effects. For lower Re, however, an inertial-range model can over-predict fluctuations by as much as 300%. As a cautionary reminder, it is important to remember that C_0 is not known with any certainty and that the work in this paper does not establish the value of the inertial-range universal constant unambiguously. The work does favour a larger C_0 value, say $C_0 \sim 6$, but there is no precision in this estimate.

Figure 14 shows the variation of the concentration fluctuations for various C_0 produced by Thomson's inertial-range model (i.e. our model with infinite Pe and Re). The source size is $\sigma_0 = 0.01$. The magnitude of the fluctuations varies by as much as a factor of 2 across the range of uncertainty of C_0 (say $2 \leqslant C_0 \leqslant 10$) thus it is clear that the value of C_0 is an important determinant in Lagrangian modelling. It should be noted that the work in this paper, while favouring a value in excess of 6, does not provide a new reliable estimate of the important inertial-range quantity C_0.

Also, although we find that Thomson's model performs well for the purposes of the

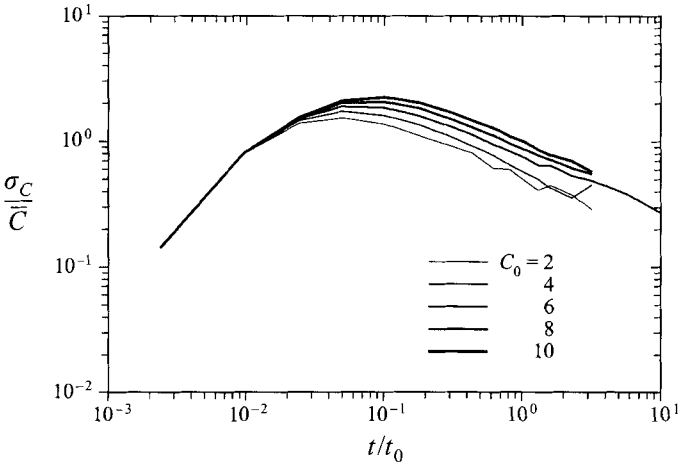

FIGURE 14. Normalized centreline concentration fluctuations given by Thomson's inertial-range model for inviscid self-similar decaying turbulence ($m = 0.7$). The curves are for a sequence of ever-larger $\tilde{C}_0$ values. The source size is $\sigma_0/L_0 = 0.01$.

finite-Pe comparison, the sensitivity of the results to the form of $\boldsymbol{a}$ in the velocity equation is reduced when molecular effects are important. In the limit of large Pe, when the small-scale turbulent motions are the sole means for separating fluid particles, it would be worthwhile to reconsider the velocity drift term in more detail, as in Borgas & Sawford (1994*b*).

8. Discussion

We have developed a stochastic model for relative dispersion which takes account of molecular diffusion and viscous dissipation ranges, the latter in an *ad hoc*, but physically reasonable, way. Despite the approximations and uncertainties, this model represents a very advanced and useful tool for examining concentration fluctuations in turbulent flows. Such fluctuations are then considered, with particular emphasis on a new data set available to the authors. An encouraging degree of agreement is found between the measurements and simulations: the mean-concentration field was used to fit a model parameter and then the concentration fluctuations are calculated with no further free parameters. Fluctuations along the plume centre line agree in magnitude to about 30% (although often better), but the shape of the curve varying from close to the source to far downstream is very well represented by the processes included in modelling. The off-centreline variation of the fluctuations is also well represented by the model, thereby giving a model for the entire concentration-fluctuation field from a line source. The quantitative agreement available here is much more satisfactory than when viscosity and molecular diffusivity are ignored.

The model is also used for a sequence of increasing Re values and shows practical convergence to an $Re = \infty$ inertial-range model when $Re \approx 10^4$. Thus for most atmospheric applications an inertial-range model, such as Thomson's (1990) model, is adequate.

Source-size effects can be better examined with the new model (particularly for sources with scale of order η) and comparisons show that the molecular effects diminish as the source becomes larger. Sources with scales η and smaller essentially give the same fluctuation intensities, which is not the case if a non-truncated inertial-range model is used.

An important characteristic of our model is the tendency for finite-Re models to overshoot the infinite-Re predictions of fluctuation intensities (molecular diffusion initially decreases the intensity of fluctuations). This reflects a dominant tendency of viscous effects to force particle pairs to remain close together despite the dual action of molecular diffusion and turbulent eddies separating them. Of course, pairs are eventually rent apart, but it is significant to observe that this effect takes a considerable time to affect the fluctuation intensities.

Considering all the idealizations and approximations, the present level of agreement is all that can be expected. For our purposes, we feel that two-particle stochastic models of relative dispersion are vindicated by this work and it is not necessary, or useful, to strive for greater agreement between the present model (by relaxing idealizations for example) and the experiments. The ultimate goal of finding a suitable model for atmospheric dispersion, if only for much larger-Re isotropic flows, requires assessment of more suitable forms of $\boldsymbol{a}$ and more reliable estimates for C_0, but can usefully ignore explicit dissipative effects.

REFERENCES

ANAND, M. S. & POPE, S. B. 1985 Diffusion behind a line source in grid turbulence. *Turbulent Shear Flows*, vol. 4. Springer.

BORGAS, M. S. 1996 Models of material particle trajectories in turbulent flows. (In preparation.)

BORGAS, M. S. & SAWFORD, B. L. 1991 The small-scale structure of acceleration correlations and its role in the statistical theory of turbulent dispersion. *J. Fluid Mech.* **228**, 295–320.

BORGAS, M. S. & SAWFORD, B. L. 1994*a* Stochastic equations with multifractal increments for modelling turbulent dispersion. *Phys. Fluids* A **6**, 618–633.

BORGAS, M. S. & SAWFORD, B. L. 1994*b* A family of models for two-particle dispersion in isotropic homogeneous stationary turbulence. *J. Fluid Mech.* **279**, 66–99.

DURBIN, P. A. 1980 A stochastic model of two-particle dispersion and concentration fluctuations in homogeneous turbulence. *J. Fluid Mech.* **100**, 279–302.

DURBIN, P. A. 1982 An analysis of the decay of temperature fluctuations in isotropic turbulence. *Phys. Fluids* **25**, 1328–1332.

GAD-EL-HAK, M. & MORTON, J. B. 1979 Experiments on the diffusion of smoke in isotropic turbulent flow. *AIAA J.* **17**, 558–562.

KAPLAN, H. & DINAR, N. 1988 A three-dimensional stochastic model for concentration fluctuation statistics in isotropic homogeneous turbulence. *J. Comput. Phys.* **79**, 317–335.

NAKAMURA, I., SAKAI, Y. & MIYATA, M. 1987 Diffusion of matter by a non-buoyant plume in grid-generated turbulence. *J. Fluid Mech.* **178**, 379–403.

NELKIN, M. & KERR, R. M. 1981 Decay of scalar variance in terms of a modified Richardson law for pair dispersion. *Phys. Fluids* **24** (9), 1754–1756.

POPE, S. B. 1994 Lagrangian PDF methods for turbulent flows. *Ann. Rev. Fluid Mech.* **26**, 23–63.

RODEAN, H. C. 1991 The universal constant for the Lagrangian structure function. *Phys. Fluids* A **3**, 1479–1480.

SAFFMAN, P. G. 1960 On the effect of the molecular diffusivity in turbulent diffusion. *J. Fluid Mech.* **8**, 273–283.

SAWFORD, B. L. 1983 The effect of Gaussian particle-pair distribution functions in the statistical theory of concentration fluctuations in homogeneous turbulence. *Q. J. R. Met. Soc.* **109**, 339–354.

SAWFORD, B. L. 1991 Reynolds number effects in Lagrangian stochastic models of dispersion. *Phys. Fluids* A **3**, 1577–1586.

SAWFORD, B. L. & BORGAS, M. S. 1994 On the continuity of stochastic models for the Lagrangian velocity in turbulence. *Physica* D **76**, 297–311.

SAWFORD, B. L. & HUNT, J. C. R. 1986 Effects of turbulence structure, molecular diffusion and source size on scalar fluctuations in homogeneous turbulence. *J. Fluid Mech.* **165**, 373–400.

SAWFORD, B. L. & TIVENDALE, C. 1992 Measurement of concentration statistics downstream of a line source in grid turbulence. *Proc. 11th Australasian Fluid Mech. Conf. Hobart*, vol. 2, pp. 945–948.

SINIA, YA. G. & YAKHOT, V. 1989 Limiting probability distribution of a passive scalar in a random velocity fluid. *Phys. Rev. Lett.* **63**, 1962–1964.

STAPOUNTZIS, H., SAWFORD, B. L., HUNT, J. C. R. & BRITTER, R. E. 1986 Structure of the temperature field downwind of a line source in grid turbulence. *J. Fluid Mech.* **165**, 401–424.

THOMSON, D. J. 1987 Criteria for the selection of stochastic models of particle trajectories in turbulent flows. *J. Fluid Mech.* **180**, 529–556.

THOMSON, D. J. 1990 A stochastic model for the motion of particle pairs in isotropic high Reynolds number turbulence, and its application to the problem of concentration variance. *J. Fluid Mech.* **210**, 113–153.

TOWNSEND, A. A. 1954 The diffusion behind a line source in homogeneous turbulence. *Proc. R. Soc. Lond.* A **224**, 487–512.

UBEROI, M. S. & CORRSIN, S. 1952 Diffusion of heat from a line source in isotropic turbulence. *National Advisory Committee for Aeronautics Tech. Note* 2710.

WARHAFT, Z. 1984 The interference of thermal fields from line sources in grid turbulence. *J. Fluid Mech.* **144**, 363–387.

YEUNG, P. K. & POPE, S. B. 1989 Lagrangian statistics from direct numerical simulations of isotropic turbulence. *J. Fluid Mech.* **207**, 531–586.